RSC Advances

PAPER

View Article Online
View Journal | View Issue

Cite this: *RSC Adv.*, 2017, **7**, 37908

Examining the molecular entanglement between V=O complexes and their matrices in atmospheric residues by ESR

Qingyan Cui,[a] Koji Nakabayashi,[a] Xiaoliang Ma,[b] Keiko Ideta,[a] Jin Miyawaki,[a] Abdulazim M. J. Marafi,[b] Adel Al-Mutairi,[b] Joo-Il Park,[b] Seong-Ho Yoon[a] and Isao Mochida*[c]

The V=O complexes in atmospheric residues (ARs) and their maltene, resin and asphaltene fractions have been investigated using ESR to examine the effects of the surrounding matrices, measurement temperature, pre-heat-treatment of AR as well as addition of toluene on the electron structure and mobility of the V=O ion. The *B* parameter calculated on the basis of the ESR spectrum has been found to be a good index to reflect the molecular entanglement between the V=O complexes and their matrixes in ARs and their fractions, and to indicate the effects of the measurement temperature, pre-heat-treatment as well as the solvent on such interactions. The *B* parameter value for the V=O complexes decreases in the order of asphaltenes > AR ≈ resins > maltenes, implying that the constraint on the mobility of the V=O complexes in the samples decreases in the same trend. Increasing temperature, pre-heat-treatment and the addition of toluene reduce the *B* parameter value, thus, favoring the mobility of the V=O complexes in the ARs and their fractions. It can be ascribed to the change in the peripheral environment of the V=O complexes surrounded by the matrix molecules. A comprehensive understanding of such molecular entanglement between the V=O complexes and their matrixes in ARs may give some important hints to improve the hydrodemetallization performance of AR.

Received 8th June 2017
Accepted 21st July 2017

DOI: 10.1039/c7ra06436e

rsc.li/rsc-advances

1. Introduction

Vanadium(v) and nickel (Ni) in petroleum have been targets of extensive research, since such metals always poison the hydrodesulfurization (HDS), hydrodenitrogenation (HDN) and hydrocracking catalysts in refining processes through depositing on the catalyst surface, resulting in decreasing the catalyst activity and shortening the catalyst lifetime.[1–4] Hence, it is highly desirable to improve the metal removal performance in the hydrodemetallization (HDM) process.

It is very significant to fully understand the molecular structure and physicochemical properties of the metal complexes, as well as their relationships with surrounding molecules in petroleum for designing a better HDM catalyst and a more efficient HDM process. Vanadyl (V=O) and nickel porphyrins are the common and major metal species in petroleum, although some non-porphyrin V and Ni species were also found in petroleum.[5,6] The metal complexes in petroleum have been widely studied.[7–9] The form of the V=O complexes in the different fractions of Mayan asphaltenes has been studied by X-ray absorption spectroscopy.[10] The peripheral substitution of the porphyrin macrocycle can be examined by using the ultraviolet/visible absorption spectroscopy.[11] Shi *et al.* clarified the structures of the V=O porphyrins in the crude oil by FT-ICR-MS.[12,13] Biktagirov *et al.* studied the structure of vanadyl porphyrin in crude oil by electron–nuclear double resonance (ENDOR).[14] However, there is few report about how these V=O porphyrins are associated with their surrounding organic matrix in petroleum, which may affect the approach of the porphyrins to the active phase on HDM catalyst surface, and thus has an impact on their HDM activity.

The major metal complexes exist in the polar fractions (resins and asphaltenes), especially in asphaltenes.[15,16] Yen and his group[17–19] proposed a trapping model of the metal complexes in the resins and asphaltenes through physical and covalent bonding, indicating that the metal complexes may behave together with their matrix molecules and aggregation. Ideally, the metal complexes are released from their matrixes to reach freely to the surface of the HDM catalyst. In GC-AED[20] and FT-ICR-MS,[21,22] the metal complexes are vaporized and ionized, where the metal complexes can be released from their matrixes through thermal or photo-electronic effect. Thus it is very important to clarify the molecular entanglement between the metal complexes and their matrixes or their aggregates in AR.

[a]*Institute for Materials Chemistry and Engineering, Kyushu University, Kasuga, Fukuoka, Japan*

[b]*Petroleum Research Center, Kuwait Institute for Scientific Research, Safat, Kuwait*

[c]*Kyushu Environmental Evaluation Association, Fukuoka, Japan. E-mail: mochida@keea.or.jp; Tel: +81-092-662-0410*

Electron Spin Resonance (ESR) has been applied to analyse V=O complexes in petroleum to extract information on their structure and mobility.[23–28] Wong and Yen proposed that the mobility of the V=O complexes can be defined by using ESR to distinguish anisotropic/isotropic spectrum of the V=O complexes.[29] It is assumed that the anisotropic spectrum reflects the constraint of V=O complexes in petroleum fractions. The differently constrained extent gives different type of ESR spectrum.[29] Campbell and Freed[30] concluded that the rotational mobility of the V=O complex gives the anisotropic or isotropic spectrum according to its rotational rate. They reproduced a series of spectra by simulation based on the perturbation theory applying rotational correlation time (τ_R) in Brownian diffusion model and the residual line width contribution.

ESR has also been used for identifying vanadium environment in petroleum by examining g values and hyperfine coupling constants for several square pyramidal environments on the vanadyl complex.[31] Espinosa *et al.* provided a deeper analysis of the electron structure of the vanadyl complex in a series of natural porphyrins in the heavy crude oil through the ESR measurement.[32] They estimated relative strength of the V–N bonds in the ligand and the V=O bond through the delocalization of the unpaired electrons on V^{4+} to the coordinating nitrogen. In our previous paper,[33] behaviors of the V=O complexes in atmospheric residues, their resins and asphaltenes in the presence of the solvents (toluene or tetrahydrofuran) were studied by ESR in detail at 20 to 100 °C to examine the effects of surrounding matrix, concentration in solvent and temperature on the V=O rotational mobility. However, the direct examination of the molecular entanglement between the V=O complexes and their matrixes in the real ARs and their fractions in the absence of the solvent, which has more application value, has not been involved yet.

In the present study, the electron structure and mobility of V=O in three atmospheric residues and their fractions in the absence of the solvent were studied by ESR through the comparison of the ESR parameter B, which is a sensitive indicator to the electron structure of V=O[32] and the effect of measurement temperature, pre-heat-treatment as well as the solvent of toluene on the V=O electron structure were examined to clarify the molecular entanglement between the V=O complexes and their surrounding molecules.

2. Experimental

2.1. Sample preparation

Two kinds of atmospheric residues (AR) from Lower Fars crude and Kuwait export crude (LF-AR and KEC-AR), respectively, were used in this study. LF-AR and KEC-AR were blended at a ratio of 1/1 (g g^{-1}) at 20 °C to obtain the mixed AR (LF/KEC-AR). Some compositions and properties of these ARs are listed in Table 1. The data clearly indicates that the AR becomes heavier in the order of KEC-AR < LF/KEC-AR < LF-AR. The LF-AR was heat-treated in an autoclave at 330 °C under a hydrogen pressure of 9 MPa for 3 h to prepare the heat-treated AR. The heat-treated LF-AR, its resins and asphaltenes named as HT-LF-AR, HT-LF-R and HT-LF-As, respectively.

Table 1 Properties of three ARs

	LF-AR	KEC-AR	LF/KEC-AR
Boiling point (°C)	>360	>360	>360
Density (g ml^{-1})	1.0081	0.9745	0.9873
C (wt%)	82.6	83.8	83.4
H (wt%)	10.1	11.0	10.5
S (wt%)	3.44	3.19	3.34
N (wt%)	0.33	0.29	0.32
V (ppm)	152	71	108
Ni (ppm)	24	14	20
Saturate (wt%)	16.7	25.7	20.7
Aromatics (wt%)	51.9	48.8	50.2
Resin (wt%)	19.5	18.4	19.2
Asphaltene (wt%)	11.9	7.2	9.9

The maltene, resin and asphaltene fractions from the ARs were obtained by the fractionation shown below: AR was dissolved in n-heptane at a weight ratio of 1/50 (g g^{-1}) with stirring at 60 °C for 5 h, and then the mixture was filtered. The insoluble fraction was extracted in the Soxhlet apparatus with toluene until the extraction solvent became no color, and the solution was rotary-evaporated to recover the asphaltene fraction, which is in the fine powder form. The maltene fraction was obtained by removing n-heptane from the n-heptane solution in a rotary evaporator. The obtained maltene fraction was further fractionated by chromatographic separation in a glass column packed with activated neutral alumina. The maltene fraction with a little amount of n-hexane was poured into the top of the glass column, and then was eluted consecutively with n-heptane, toluene and toluene/methanol mixture (9 : 1, v/v) with a ratio of solvent to maltene of 250 ml to 1 g for each solvent. The received solutions were rotary-evaporated to obtain the saturate, aromatic and resin fractions, respectively. The resin fraction is in the solid form.

2.2. Electron spin resonance analysis

All spectra of ESR were recorded on a JESFA200 ESR spectrometer with an X-band Bridge (JEOL Ltd., Tokyo, Japan) using standard 100 kHz field modulation. The sample was measured at a microwave frequency of 9.0 GHz and power of 1.0 mW with a cylindrical TE cavity, and the magnetic field was calibrated using Mn^{2+} powder as an ESR marker. A temperature accessory (DVT controller, JEOL) was used to control the measurement temperature of the sample in the cavity. The quartz tube (5 mm o.d., 4 mm i.d.) was used to hold sample, which was inserted along the cylindrical axis of the cavity. The ARs, heat-treated LF-AR, their resins and asphaltenes were investigated at different temperatures by ESR, as well as the LF-AR, its resin and asphaltene fractions dissolved in toluene (Wako Chemicals, Tokyo Japan) at a concentration of 20 wt% were examined for ESR analysis.

The B parameter has been used as a sensitive indicator of the tetragonal distortion to clarify a change in the V=O bond length and distance of four nitrogen ligands in the basal plane, as reported in the literature,[32] which can be derived as follows:

$$B = \Delta g_{\parallel}/\Delta g_{\perp}$$

$$\Delta g_{\parallel} = g_{\parallel} - g_{e}$$

$$\Delta g_{\perp} = g_{\perp} - g_{e}$$

where $g_{\parallel}$ and $g_{\perp}$ values are associated with the magnetic field, which are used as parameters for the vanadyl complexes to clarify the vanadium electronic structure. g_e is the free electron g value of 2.0023.

The method for studying the vanadyl complexes through the parameter values from the ESR analysis has been described in detail in the literatures.[25,32] The relative parameter values are obtained using anisotropic simulation software (JEOL Ltd., Tokyo, Japan), and the deviation for $g_{\parallel}$, $g_{\perp}$ and B is 0.0003, 0.0001 and 0.05, respectively.

3. Results

3.1. Effect of surrounding matrixes on V=O electron structure

Fig. 1 shows the ESR spectra of V=O complexes in LF-AR, KEC-AR and LF/KEC-AR measured at 20 °C. All of V=O complexes in the three ARs displayed anisotropic spectra with very slow mobility, indicating that the V=O complexes in the ARs can hardly rotate in the magnetic field due to the strong constraint of the surrounding molecules.[17,23,34] No significant difference was observed directly from the comparison of the ESR spectra for the three ARs. Consequently, the B parameter was used as an indicator in the present study to describe the change of the V=O electron structure, as it may be more sensitive to the changes of the V=O electron structure.[32] Various ESR parameters for V=O in ARs and their maltene, resin and asphaltene fractions measured at 20 °C are summarized in Table 2. Although the differences in B parameter values for the V=O in LF-AR, KEC-AR and LF/KEC-AR, as well as their maltene, resin and asphaltene fractions were small, the B parameter values for V=O complexes in KEC-AR and their fractions were clearly smaller than those in LF-AR and their fractions. The LF/KEC-AR displayed B parameter value that was almost the same as the average value of LF-AR and KEC-AR, which indicates that the blending has almost no synergetic effect on the change of V=O electron structure at this condition.

Table 2 ESR parameters of V=O complexes in ARs, maltenes, resins and asphaltenes at 20 °C

Samples		$g_{\parallel}$	$g_{\perp}$	B
ARs	LF	1.9615	1.9943	5.10
	KEC	1.9615	1.9942	5.04
	LF/KEC	1.9618	1.9943	5.06
Maltenes	LF	1.9618	1.9943	5.06
	KEC	1.9616	1.9941	4.96
	LF/KEC	1.9616	1.9942	5.02
Resins	LF	1.9619	1.9944	5.11
	KEC	1.9614	1.9942	5.05
	LF/KEC	1.9616	1.9943	5.09
Asphaltenes	LF	1.9617	1.9945	5.21
	KEC	1.9615	1.9944	5.16
	LF/KEC	1.9615	1.9944	5.16

Fig. 2 displays the ESR spectra of V=O complexes in LF-AR and its maltene, resin and asphaltene fractions measured at 20 °C. The ESR spectra of LF-AR, LF-Mal, LF-R and LF-As were similar, showing anisotropic spectra. Similarly, it is hard to observe the difference of V=O complexes stage in these samples by comparing the ESR spectra at this condition. However, the B parameter value of the V=O in asphaltene fraction was slightly, but definitely, larger than those in the AR and its maltene and resin fractions, regardless of the three ARs, as shown in Table 2, indicating a shorter V=O bond and/or a longer distance to the nitrogen ligands, *i.e.*, the higher electron density in the axial bond and more electron delocalization to the V orbital are suggested.[32] It implies that a larger degree of constraint to the mobility of V=O complexes by the surround molecules (matrixes) was found in asphaltene fraction.

The ESR spectra were obtained at 150 °C for V=O complexes in LF-AR, its maltenes, resins and asphaltenes, as shown in Fig. 3, further confirm this constraint by the matrixes. V=O complexes in LF-maltenes gave a different spectrum, which corresponds to that of TPP V=O complex dissolved in toluene measured at −105 °C, while the spectra of V=O complexes in LF-AR, LF-resins and LF-asphaltenes correspond to that of TPP

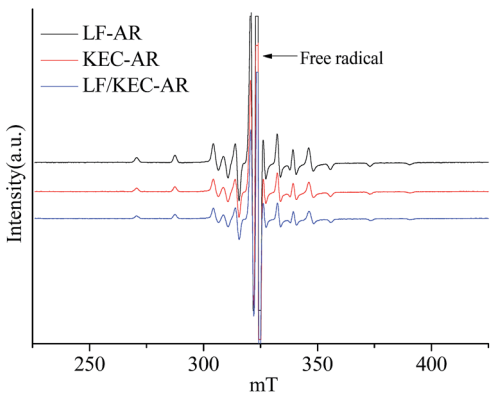

Fig. 1 ESR spectra of V=O complexes in ARs at 20 °C.

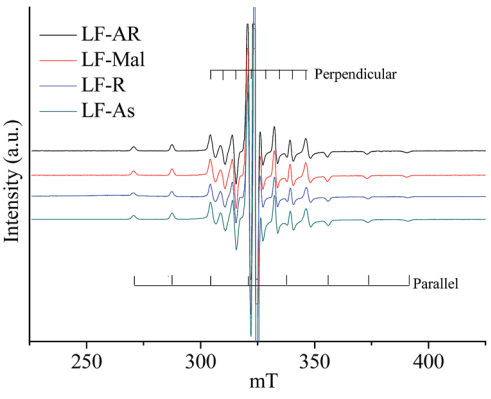

Fig. 2 ESR spectra of V=O complexes in LF-AR, maltenes, resins and asphaltenes at 20 °C.

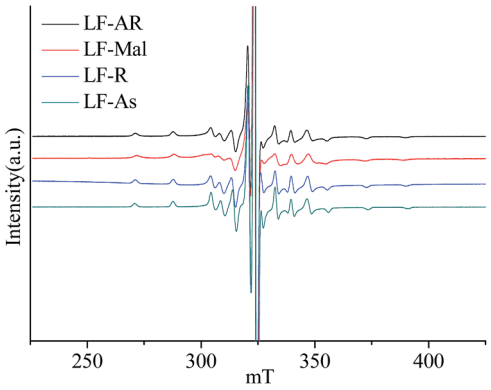

Fig. 3 ESR spectra of V=O complexes in LF-AR, its maltenes, resins and asphaltenes at 150 °C.

V=O complex dissolved in toluene measured at −120 °C, which was reported in the previous paper.[33] It indicates that the mobility of V=O complexes in LF-maltenes was rapider than those in other samples at this measurement condition.[17,23] The *B* parameter value of V=O in asphaltenes was also significantly larger than those in AR and resins measured at 150 °C. It is clearly shown that the constraint of the V=O complexes by the surrounding molecules was in the order of maltenes < resins ≈ AR < asphaltenes.

3.2. Effect of the measurement temperatures on V=O electron structure

The ESR parameter values of V=O complexes in LF-AR, its resins and asphaltenes measured at 20, 50 and 150 °C are summarized in Table 3. The values of parameters $g_{\|}$, $g_{\perp}$ and *B* for V=O complexes in LF-AR, LF-R and LF-As measured at 50 °C were similar with those at 20 °C, respectively, indicating no significant effect on the V=O electron structure when the temperature increased from 20 to 50 °C. When the measurement temperature was further raised to 150 °C, the $g_{\perp}$ values for V=O complexes in LF-AR, LF-R and LF-As decreased, resulting in an obvious reduction of *B* values to 4.14, 4.09 and 4.80, respectively, although their ESR spectra were still anisotropic. It indicates that the increase in temperature changed the V=O electron structure due to weakening the interaction between the V=O complexes and their surrounding molecules.

Table 3 ESR parameters of V=O complexes in LF-AR, its resins and asphaltenes at different temperatures

Samples		$g_{\|}$	$g_{\perp}$	*B*
20 °C	LF-AR	1.9615	1.9943	5.10
	LF-R	1.9619	1.9944	5.11
	LF-As	1.9617	1.9945	5.21
50 °C	LF-AR	1.9615	1.9943	5.10
	LF-R	1.9616	1.9941	4.96
	LF-As	1.9615	1.9944	5.16
150 °C	LF-AR	1.9613	1.9924	4.14
	LF-R	1.9612	1.9922	4.07
	LF-As	1.9605	1.9936	4.80

3.3. Effect of the heat-treatment on the V=O electron structure

Fig. 4 illustrates ESR spectra of V=O complexes in the heat-treated LF-AR, its resins and asphaltenes measured at 150 °C. The estimated values of the ESR parameters for V=O in the heat-treated LF-AR, its resins and asphaltenes measured at 50 and 150 °C are summarized in Table 4. The heat-treated LF-AR, its resins and asphaltenes presented anisotropic spectra, similar to those of the corresponding non-heat-treated samples. However, *B* parameter values for the heat-treated LF-AR, its resins and asphaltenes were smaller than those for the non-heat-treated ones, indicating a longer of V=O bond and/or a shorter of the distance to the nitrogen ligands in the heat-treated samples.[32] The observed change in the V=O electron structure can be ascribed to that the heat-treatment moderated the constraint by the periphery environment on the V=O complexes.

3.4. Effect of solvent on the V=O electron structure

Fig. 5 displays the ESR spectra of V=O complexes in LF-AR, its resins and asphaltenes dissolved in toluene with the sample concentration of 20 wt% measured at 20 °C. The V=O complexes in the LF-AR, its resins and asphaltenes dissolved in toluene provided still slow tumbling spectra, corresponding to the spectra of TPP V=O complex dissolved in toluene measured at −105, −105 and −110 °C, respectively, which were reported in the previous paper.[33] Toluene appears to enhance the

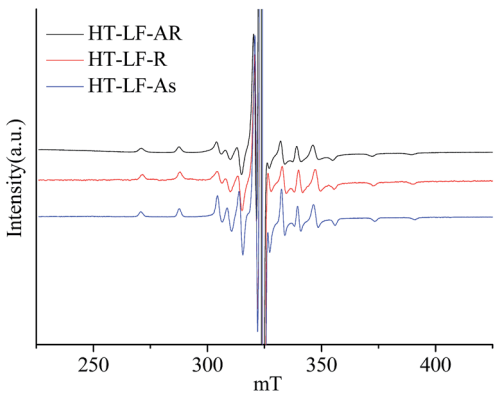

Fig. 4 ESR spectra of V=O complexes in heat-treated LF-AR, its resins and asphaltenes at 150 °C.

Table 4 ESR parameters of V=O complexes in the heat-treated LF-AR, its resins and asphaltenes

Samples		$g_{\|}$	$g_{\perp}$	*B*
50 °C	HT-LF-AR	1.9615	1.9941	4.98
	HT-LF-R	1.9612	1.9938	4.84
	HT-LF-As	1.9611	1.9942	5.09
150 °C	HT-LF-AR	1.9614	1.9922	4.05
	HT-LF-R	1.9613	1.9917	3.87
	HT-LF-As	1.9606	1.9935	4.74

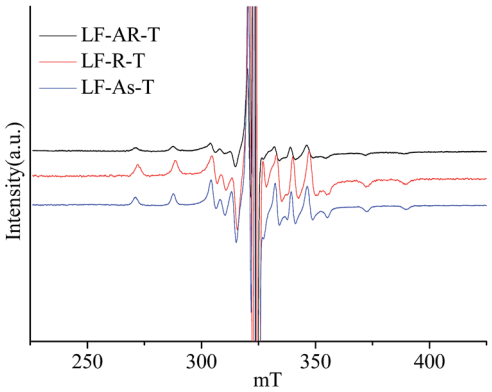

Fig. 5 ESR spectra of V=O complexes in LF-AR, its resins and asphaltenes dissolved in toluene measured at 20 °C.

Table 5 ESR parameters of V=O complexes in LF-AR, its resins and asphaltenes dissolved in toluene

Samples		$g_{\parallel}$	$g_{\perp}$	B
AR	LF	1.9615	1.9943	5.10
	LF-T	1.9628	1.9925	4.03
Resins	LF	1.9619	1.9944	5.11
	LF-T	1.9633	1.9924	3.94
Asphaltenes	LF	1.9617	1.9945	5.21
	LF-T	1.9625	1.9929	4.23

tumbling rate of V=O complexes in the samples, possibly due to the solvation of toluene reducing the constraint on the V=O complexes. The ESR parameter values for V=O in LF-AR, its resins and asphaltenes in toluene measured at 20 °C are listed in Table 5. The V=O complexes in the presence of toluene presented the larger $g_{\parallel}$ value and the smaller $g_{\perp}$ value in comparison with those in the absence of toluene, regardless of LF-AR, resins and asphaltenes. It indicates that the V=O electron structure was obviously changed by the solvent effect of toluene.

4. Discussion

4.1. The constraint on V=O complexes in ARs and their fractions

The V=O complexes in AR and its maltenes, resins and asphaltenes measured at 20 °C give anisotropic spectra with 16 lines hyperfine structure, as shown in Fig. 2, which corresponds to that of TPP V=O complex dissolved in toluene at measured −120 °C.[33] AR and maltene fraction are liquid of high viscosity, while the resin and asphaltene fractions are solid, all of them give similar ESR spectra with very slow tumbling rate, regardless of their states, indicating very strong constraint on the V=O complexes by the surrounding matrix, resulting in the very slow rotation of the V=O complexes.[17,23,34]

However, the B parameter is sensitive to the electron structure of V=O, thus it is used in the present study to describe the change of V=O electron structure in AR and its fractions to clarify the molecular entanglement between the V=O complexes and their surrounding molecules. The B parameter value for V=O in LF-AR is slightly larger than that in KEC-AR. For the samples of AR, maltenes, resins and asphaltenes measured at 20 °C, the B parameter value decreases in the order of asphaltenes > AR ≈ resins > maltenes. The larger B parameter value reflects shorter length of V=O bond and/or a longer of the distances to the nitrogen ligands, which is caused by the higher electron density in the axial bond and larger electron delocalization to the V orbital due to the charge transfer from the π system of the porphyrin ring.[32] The larger aromatics group bonding with the porphyrin ring in the heavy AR or its fractions may transfer more charge from the extended π system, resulting in the larger electron delocalization, particularly when the aromatic sheets are stacked.[26,35] Thus, the larger B parameter value indicates the stronger constraint on the V=O complexes by the surrounding matrix.

At 150 °C, the ESR spectrum of V=O complexes in maltenes, which consists of saturate, aromatic and resin fractions without asphaltenes, shows a little rapider mobility in comparison with those in AR and its resin and asphaltene fractions. Since asphaltene fraction is free from saturate, aromatic and resin fractions, the mobility of the V=O complexes in the asphaltene fraction is constrained strongly by itself (the most heavy fraction), while the aromatic fraction benefits the mobility of V=O complexes in the maltenes. Mutual interaction among the fractions is fatal for the mobility of V=O complexes present in the real AR (a mixture of the fractions).

4.2. Moderation of constraint on V=O complexes

The V=O complexes in LF-AR and its fractions at 20 and 150 °C shows similar ESR spectra, except for those in the maltene fractions at 150 °C. However, the B parameter value decreases as the measurement temperature raises, indicating a lengthening of the V=O bond and/or a shortening of the distances to the nitrogen ligands. The higher temperature may moderate the constraint force of the matrix molecules on the V=O complexes, even if they are still trapped. The difference between the B parameter values for the resin and asphaltene fractions increases significantly with increasing measurement temperature, possibly due to larger entropy contribution. It suggests that the change of V=O electronic structure in the resin fraction is more obvious, which can be ascribed that the effect of the higher measurement temperature on moderating the constraint on the V=O complexes by their surrounding matrix in resin fraction is larger than that in asphaltene fraction because of the weaker aggregation in the former.

The heat-treated AR and its resin and asphaltene fractions provide the smaller B parameter values compared with the non-heat-treated ones. The heat-treatment at 330 °C under a hydrogen pressure of 9 MPa for 3 h shifted the V=O complexes from asphaltenes to resins, and decreased the amount of V=O complexes in the heavy sub-fraction of asphaltenes, as reported in the previous paper.[16] Thus such smaller B parameter value is possibly contributed to a change in interaction between the V=O complexes and their surrounding matrix in AR and asphaltenes during the heat-treatment process, which results in the change of the V=O electron structure.

When the V=O complex was dissolved in solvent, it gave isotropic spectrum, as observed for the standard V=O complex dissolved in toluene.[33] However, in the present study, LF-AR and its resin and asphaltene fractions dissolved in toluene with the concentration of 20 wt%, although presenting in a kind of soluble form give anisotropic spectra at the same measurement condition. Nevertheless, the spectra of LF-AR and its resin and asphaltene fractions indicate that the solvent of toluene certainly enhances the mobility of V=O. In addition, the *B* parameter values for the V=O in LF-AR and its resin and asphaltene fractions dissolved in toluene are obviously smaller than those without toluene. Thus, toluene, which solvates the resins and asphaltenes, loosens the interaction between the V=O complexes and the surrounding molecules in the matrix, and causes the change of the V=O electron structure. The V=O complexes in LF-AR and its resin and asphaltene fractions dissolved in toluene are still trapped by the surrounding molecules, because they still show anisotropic spectra. How to release the V=O complexes from their matrix in AR will be a further research topic. A important message got from this study is to reduce the constraint by the surrounding matrix on the V=O complexes through some effective way, which will favour the approach of the V=O complexes freely to the catalyst surface and/or into the catalyst pore, and thus benefit the metal removal and reduction of the coke formation on the HDM catalyst.

5. Conclusions

The *B* parameter calculated on the basis of the ESR spectra is found to be a good index to reflect the molecular entanglement between the V=O complexes and their matrix in ARs and their fractions, and to indicate the effects of the measurement temperature, pre-heat-treatment and the solvent on such interaction. The *B* parameter value for the V=O complexes decreases in the order of asphaltenes > AR ≈ resins > maltenes, implying that the constraint on the mobility of the V=O in the samples decreases in the same trend. Increasing temperature, pre-heat-treatment and the addition of toluene reduce the *B* parameter value, then thus, favour the mobility of the V=O complexes in the ARs and their fractions. It is ascribed to the change in the peripheral environment of the V=O complexes surrounded by the matrix molecules. Hence, the *B* parameter can be used as an index to define the nature and state of the V=O complexes, being expected to reflect the HDM reactivity of AR. The way to increase the HDM reactivity of ARs may be assessed on the basis of the change in the *B* parameter value according to the measured ESR spectra.

Acknowledgements

The authors acknowledge Japan Cooperation Center Petroleum (JCCP), the Kuwait Oil Company (KOC) and the Kuwait Institution for Scientific Research (KISR) for supporting on this joint project. Acknowledgement is also extended to Kuwait National Petroleum Company (KNPC) for the in-kind contribution and technical support.

References

1 C. D. Pearson and J. B. Green, *Energy Fuels*, 1993, **7**, 338–346.
2 F. G. Lepri, B. Welz, D. L. Borges, A. F. Silva and M. G. Vale, *Anal. Chim. Acta*, 2006, **558**, 195–200.
3 A. Hausera, A. Stanislausb, A. Marafib and A. Al-Adwani, *Fuel*, 2005, **84**, 259–269.
4 M. S. Rana, J. Ancheyta, S. K. Sahoo and P. Rayo, *Catal. Today*, 2014, **220–222**, 97–105.
5 E. W. Baker, T. F. Yen, J. P. Dickie, R. E. Rhodes and L. F. Clark, *J. Am. Chem. Soc.*, 1967, **89**, 3631–3639.
6 J. M. Sugihara and R. M. Bean, *J. Chem. Eng. Data*, 1962, **7**, 269–271.
7 G. P. Dechaine and M. R. Gray, *Energy Fuels*, 2010, **24**, 2795–2808.
8 C. D. Pearson and J. B. Green, *Fuel*, 1989, **68**, 456–464.
9 M. Loos, I. Ascone, P. Friant, M. F. Ruiz-Lopez and L. Goulon, *Catal. Today*, 1990, **7**, 497–513.
10 J. T. Miller, R. B. Fisher, A. M. J. V. Eerden and D. C. Koningsberger, *Energy Fuels*, 1999, **13**, 719–727.
11 D. H. Freeman, D. C. S. Martin and C. J. Boreham, *Energy Fuels*, 1993, **7**, 194–199.
12 X. Zhao, Y. Liu, C. M. Xu and Q. Shi, *Energy Fuels*, 2013, **27**, 2874–2882.
13 H. Liu, J. Mu, Z. X. Wang and Q. Shi, *Energy Fuels*, 2015, **29**, 4803–4813.
14 T. Biktagirov, M. Gafurov, G. Mamin, I. Gracheva, A. Galukhin and S. Orlinskii, *Energy Fuels*, 2017, **31**, 1243–1249.
15 J. G. Reynolds, *Liq. Fuels Technol.*, 1985, **3**, 73–105.
16 Q. Y. Cui, K. J. Nakabayashi, X. L. Ma and I. Mochida, *Energy Fuels*, 2017, **31**, 6637–6648.
17 E. Tynan and T. F. Yen, *Fuel*, 1969, **43**, 191–208.
18 A. O. Barakat and T. F. Yen, *Energy Fuels*, 1989, **3**, 613–616.
19 T. F. Yen, J. G. Erdman and A. J. Saraceno, *Anal. Chem.*, 1962, **34**, 694–700.
20 T. Kim, J. Ryu and M. J. Kim, *Fuel*, 2014, **117**, 783–791.
21 A. M. McKenna, J. M. Purcell and R. P. Rodgers, *Energy Fuels*, 2009, **23**, 2122–2128.
22 K. N. Qian, K. E. Edwards and A. S. Mennito, *Anal. Chem.*, 2010, **82**, 413–419.
23 Y. Yamadat, K. Ouchi, Y. Sanada and J. Sohma, *Fuel*, 1978, **57**, 79–84.
24 K. Shibata, H. Kakiyama, Y. Sanada and J. Sohma, *Fuel*, 1979, **58**, 888–892.
25 V. M. Malhotra and H. A. Buckmaster, *Fuel*, 1985, **64**, 335–341.
26 V. Ramachandran, J. Tol, A. M. McKenna, R. P. Rodgers, A. G. Marshall and N. S. Dalal, *Anal. Chem.*, 2015, **87**, 2306–2313.
27 S. N. Trukhan, S. G. Kazarian and O. N. Martyanov, *Energy Fuels*, 2017, **31**, 387–394.
28 G. V. Mamin, M. R. Gafurov, R. V. Yusupov, I. N. Gracheva, Yu. M. Ganeeva, T. N. Yusupova and S. B. Orlinskii, *Energy Fuels*, 2016, **30**, 6942–6946.
29 G. K. Wong and T. F. Yen, *J. Pet. Sci. Eng.*, 2000, **28**, 55–64.

30 R. F. Campbell and J. H. Freed, *J. Phys. Chem.*, 1980, **84**, 2668–2680.
31 F. E. Dickson, C. J. Kunesh, E. L. McGinnis and L. Petrakis, *Anal. Chem.*, 1972, **44**, 978–981.
32 P. M. Espinosa, A. Campero and R. Salcedo, *Inorg. Chem.*, 2001, **40**, 4543–4549.
33 Q. Y. Cui, K. J. Nakabayashi, X. L. Ma and I. Mochida, *Energy Fuels*, 2017, **31**, 4748–4757.
34 T. B. Biktagirov, M. R. Gafurov, M. A. Volodin, G. V. Mamin and S. B. Orlinskii, *Energy Fuels*, 2014, **28**, 6683–6687.
35 L. Petrakis and D. W. Grandy, *Anal. Chem.*, 1978, **50**, 303–308.